08

Fabrication of dielectric resonators on the light-emitting Ge/Si heterostructures

© D.V. Yurasov,[1] M.V. Shaleev,[1] D.V. Shengurov,[1] A.V. Peretokin,[1] E.V. Skorokhodov,[1] E.E. Rodyakina,[2,3] Zh.V. Smagina,[2] A.V. Novikov[1]

[1] Institute for Physics of Microstructures, Russian Academy of Sciences,
603950 Nizhny Novgorod, Russia
[2] Rzhanov Institute of Semiconductor Physics, Siberian Branch, Russian Academy of Sciences,
630090 Novosibirsk, Russia
[3] Novosibirsk State University,
630090 Novosibirsk, Russia
e-mail: Inquisitor@ipmras.ru

Received July 12, 2024
Revised October 28, 2024
Accepted November 14, 2024

The paper presents the results of developing the technology for deep anisotropic plasma-chemical etching of semiconductor GeSi structures using inverse electron lithography with the combined deposition of a metal mask and e-beam resist. Optimization of various stages of the technological process for the formation of a metal mask and subsequent transfer of the pattern to the real structure was carried out, taking into account the proximity effect during lithography and changes in the actual sizes of holes during plasma-chemical etching. The results obtained by this method are compared with the approach of using a specialized high-contrast e-beam resist as a mask. The capabilities of this approach for the formation of two-dimensional photonic crystals on a GeSi semiconductor heterostructure with a thickness of 1 μm or above have been demonstrated. It is shown that the formed photonic crystals make it possible to increase the intensity of the photoluminescence signal by more than an order of magnitude compared to the initial structure.

Keywords: SiGe heterostructures, electron beam lithography, metal mask, reactive ion etching, photonic crystals, photoluminescence.

DOI: 10.61011/TP.2025.01.60516.229-24

Introduction

Currently, the use of various dielectric resonators is one of the effective approaches to modifying the optical properties of materials [1–4]. This approach made it possible to control the propagation of radiation on a subwavelength scale [5] and create both powerful [6] and miniature laser radiation sources [7]. The application of dielectric resonators to silicon-based structures combined with the use of modern integrated technology has led to the development of new optical elements [4,8]. This primarily applies to passive optical elements, but dielectric resonators are also used to solve the problem of creating a radiation source for silicon optoelectronics. Work is underway both towards the formation of resonators on direct-gap structures A3B5 and their integration with silicon [9,10], and the formation of resonators on light-emitting structures based on silicon [11,12] and its heterostructures with Ge [13–18]. The latter direction is more promising from the point of view of compatibility of the created radiation sources with modern integrated CMOS technology.

The Si-based dielectric microresonators (here we mean either resonators of subwavelength dimensions, or with subwavelength dimensions of elements requiring, as a rule, the use of e-beam rather than optical lithography) can be conditionally divided into two large classes built using significantly different technology. The first class includes various resonators, which most often consist of single columns of submicron size [16] or their arrays [19]. Either a mask made of a negative electron resist or a metal mask obtained using a positive electron-beam resist and lift-off lithography is used to form such resonators from planar structures by reactive ion etching. One of the main factors limiting the height of the formed resonators is the etching selectivity. Currently, negative resists based on hydrogen silsesquioxane (HSQ) provide good opportunities for creating Mie resonators. It has been demonstrated in Ref. [20] that this negative resist ensures selectivity (silicon etching rate : etching rate of the resist) of 19 : 1 in case of etching silicon in a mixture of gases $SF_6 + C_4F_8$. However, a short shelf life is a significant disadvantage of this resist (from 3 to 9 months, depending on the solvent and storage conditions [21]). An alternative approach to the formation of Mie resonators is the use of a positive electron-beam resist and a mask made of a metal film, for example, Cr film formed using lift-off lithography [22]. In this case, the low rates of Cr etching in fluoride plasma ensure a very high selectivity of etching with respect to silicon structures [23].

The second class of dielectric microresonators includes various two-dimensional photonic crystals (PhC), which are most often ordered arrays of holes of submicron diameter formed by plasma chemical etching methods [24]. A simple way to form PhC is to use a mask made of the most widely used positive resist based on polymethylmethacrylate (PMMA). However, the low ($\sim 2:1$) selectivity of PMMA etching with respect to silicon for common conditions of plasmochemical etching [25] imposes serious limitations on the PhC etching depth. It has been demonstrated that these limitations are insignificant in case of formation of PhC on „silicon on insulator " (SOI) [12] and structures with Ge(Si) self-forming nanoislands if the total thickness of the structure above the buried oxide does not exceed 350−400 nm [26].

However, light-emitting structures based on Ge layers formed on silicon have recently attracted increased attention [27–29]. Although germanium, like silicon, is a an indirect gap semiconductor, the difference between direct and indirect band gaps in it is only 136 meV [27]. Therefore, the probability of optical transitions in Ge is significantly higher than in Si, and it increases in case of application of tensile stresses to it and/or in case of heavy n-type doping [27–29], or in case of introduction of tin [30–32]. Despite the progress made using these approaches, laser generation in Ge/Si structures was achieved mainly at cryogenic temperatures [31,33]. The achievement of laser generation at 300 K has also been reported, but only at enormous pumping power thresholds ($\sim$ MW/cm^2) [28], which makes such lasers unsuitable for practical applications. Therefore, work is currently underway for improving the efficiency of radiation sources based on these structures, including through the use of dielectric resonators.

A significant difference between Ge/Si structures and structures with Ge(Si) nanoislands is their large thickness, which is $\geq 1\,\mu$m. This is attributable to the need to use a buffer layer to effectively reduce the density of threading dislocations in the Ge layer grown on Si [34–36]. On the one hand, this makes it possible to obtain Ge/Si layers with a sufficiently low surface roughness (typical RMS roughness ≤ 1 nm) and with a relatively low density of threading dislocations ($\leq 10^7$ cm^{-2}) [34–37], but, on the other hand, the large thickness of Ge/Si structures subsequently complicates the formation of microresonators with submicron characteristic element sizes on such structures. Due to the higher etching rate of Ge compared to Si in fluoride plasma, when using a mask made of PMMA resist, it is possible to achieve selectivity $\sim 3:1$, which, with standard resist thicknesses of 150−200 nm, allows the formation of PhC with a hole etching depth of 500−600 nm [38], i.e. only for $\sim 1/2$ of the thickness of Ge layer. This imposes limitations on the ability to control the radiative properties of Ge/Si structures. This paper considers various approaches (high contrast positive resist and metal mask) to the formation of photonic crystals on Ge/Si structures with large etching depth ($\geq 1\,\mu$m).

1. Results and discussion

Both test structures formed on Ge(001) substrates and Ge relaxed layers grown on SOI substrates by molecular beam epitaxy were used to test the technology of formation of PhC with deep etching. A Ge layer was deposited using two-temperature scheme during the formation of Ge/SOI structure after surface cleaning and growing of a Si buffer layer with a thickness of ~ 100 nm [34,39,40]. The total thickness of the Ge layer was about 1.1 μm. The formation of the structure was finalized by cyclic annealing like in Ref. [40]. The initial Ge/SOI structures demonstrated a luminescence signal at room temperature in the region of 1.55 μm [38] associated with direct radiative transitions in the Ge layer.

Etching of structures was performed by the method of reactive ion etching with an inductively coupled plasma source (ICP RIE) using AXIC system. Two approaches to the formation of PhC structures on Ge/SOI with etching depth of $\geq 1\,\mu$m are considered in this paper. A positive high contrast electron-beam resist AR-P 6200 (CSAR 62) (AllResist, GmbH) was used for this in the first approach, a Cr film mask obtained using a positive electron resist based on PMMA and lift-off lithography was used in the second approach. The samples with a mask made of a resist were etched in a mixture of gases SF_6/CHF_3 (the flow ratio is 3:20, the ICP source power was 700 W, and the RF source power was 30 W) at pressure 20 mTorr. Samples with a metal mask were etched in a mixture of gases SF_6/C_4F_8 (flow ratio 5:8, power ICP 700 W, power RF 60 W) at pressure 17 mTorr. These etching conditions were chosen from the point of view of either increasing the Ge etching rate while maintaining high etching anisotropy (in case of usage of a resist mask), or minimizing lateral etching (in case of usage of a metal mask). The total etching time of the structures did not exceed 2−2.5 min. The etching process was divided into stages of no more than 20 s for avoiding the overheating of the structure and the mask. Scanning electron microscopy was used to determine the parameters of the obtained PhC.

The optical properties of the formed PhC were studied using micro-PL spectroscopy at 300 K. Nd : YAG- laser (wavelength 532 nm) was used for exciting PL, the radiation of which was focused on the sample using a 10x lens and collected by the same lens. The micro-PL signal was recorded at room temperature using Bruker IFS 125 HR Fourier spectrometer and a cooled Ge detector.

The experiments using a mask made of high contrast resist AR-P 6200 resist have shown that, as stated in the specifications in Ref. [41], its etching rate is ~ 2 times smaller than the etching rate of PMMA resist under the same conditions. Only the areas of the PhC holes in which the resist is removed are etched when forming the PhC using a mask made of a resist. Therefore, to determine the depth and etching profile of the PhC holes obtained using the AR-P 6200 resist, test PhC in the form of a rectangle were formed on Ge structures, the long (length

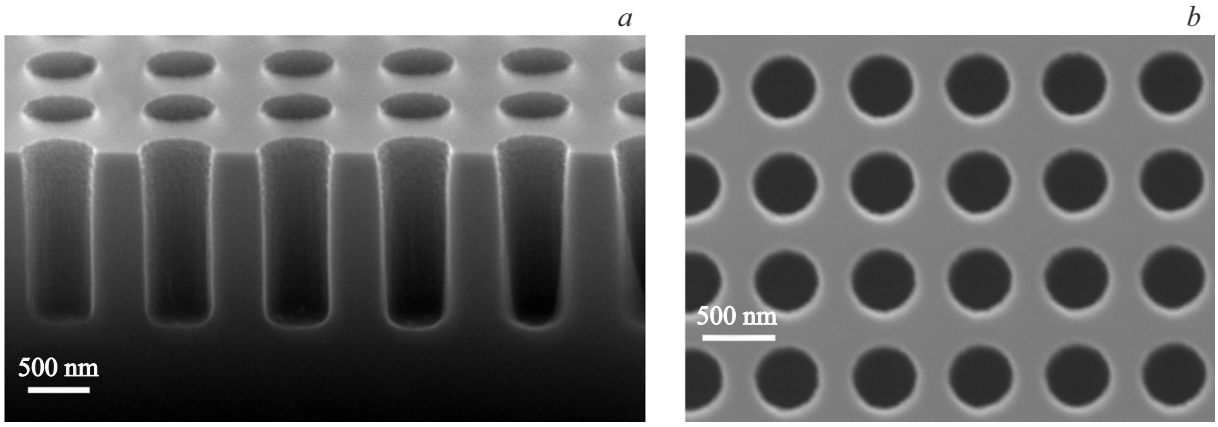

Figure 1. SEM images of one of the PhC formed on a Ge(001) wafer using a mask made of high contrast e-beam resist AR-P 6200: *a* — side view of PhC, *b* — top view of PhC.

200−300 μm) side of which was oriented perpendicular to the [110] crystallographic direction, which is the direction of light cleavage for Ge and Si plates with orientation (001). A cleavage was made across the long side of the PhC after etching, the quality of which made it possible to analyze the PhC parameters (Fig. 1, *a*). According to the analysis of SEM images, the etching depth of PhC holes decreases with the decrease of the diameter and for the studied PhC reaches $\sim 1.1\,\mu$m for holes with a diameter of ~ 300 nm and $\sim 1.5\,\mu$m for holes with a diameter of ~ 550 nm (Fig. 1). According to these data, the selectivity of etching of the structure relative to the mask was achieved in the range (6−8) : 1 during etching of Ge structures using AR-P 6200 resist mask. SEM images of PhC demonstrate high anisotropy of etching (Fig. 1, *a*) and the shape of the holes close to round (Fig. 1, *b*). Thus, using a mask made of high contrast positive electron-beam resist AR-P 6200 makes it possible to obtain PhC structures with holes of submicron diameter and etching depth $> 1\,\mu$m on Ge.

However, high cost and short (6 months [41]) shelf life is a significant disadvantage of usage of resist AR-P 6200. For this reason a chromium mask obtained using a PMMA resist mask was also used in this paper to form a PhC with a large etching depth. Chromium was chosen as the metal mask material because it has a low etching rate in fluorinated plasma [23], it can be easily applied and it is selectively removed from Si and Ge surface. The process of PhC formation using a metal mask is schematically shown in Fig. 2, *a*.

A metal mask made of Cr with a thickness of 30 nm was used in this paper. It was formed by lift off lithography method - metal deposition through a mask in a resist by magnetron sputtering, followed by removal of the unexposed resist and metal on it in dimethylformamide (90°, 60 min) (Fig. 2, *a*). A mask made of a two-layer resist PMMA950K/PMMA350K was used for the mask formation to improve the morphology of the edges of the metal mask. An artificial reverse slope of the profile of the holes in the resist is formed as a result of patterning to ensure a gap between the metal deposited in the holes on the substrate and the metal deposited on the unpatterned resist.

Unlike the formation of PhC using a positive high contrast resist, when the areas for etching PhC holes are directly patterned, when creating a metal mask using a positive resist, it is necessary to form an inverted image in it, in which not the area of the holes is patterned, but the area between the holes. It was found that, the lower the ratio of the PhC hole radius (r) to its period (a), the greater the deviation of the hole size in the metal mask from the values set in the template during lithography as a result of the proximity effect. Accordingly, the size of the obtained holes in the metal mask turns out to be noticeably smaller than the size of the holes specified in the template. Fig. 3, *a* shows the dependence of the hole size change (recalculated into the filling factor, defined as the ratio of the hole radius to their period, r/a) in a metal mask on the PhC period for three different ratios r/a (0.25, 0.3 and 0.35) nominally set in the template. It can be seen that the dependence $r/a(a)$ is linear, but its slope increases with the increase of the ratio r/a. Thus, experimentally obtained similar dependences for a given ratio r/a make it possible to predict the size of holes for other periods, but not for other ratios r/a. The sizes of the holes in the template can be recalculated to achieve the required ratios r/a based on the obtained data.

The correction factor fd to the patterning dose (base patterning dose per unit area 310 μAnd·s/cm^2, accelerating voltage 20 kV) was a variable parameter for adjusting the dimensions in the resulting mask in addition to changing the size of the hole in the template. Fig. 3, *b* shows the dependences of the hole size in the metal mask for different values of the coefficients fd (with a fixed value $r/a = 0.35$ in the template), from which it can be seen that the dependences have the same slope. Thus, the reduction of the patterning dose allows increasing the size of the holes (and, accordingly, r/a) in the mask without changing the template. However, an excessive reduction of coefficient

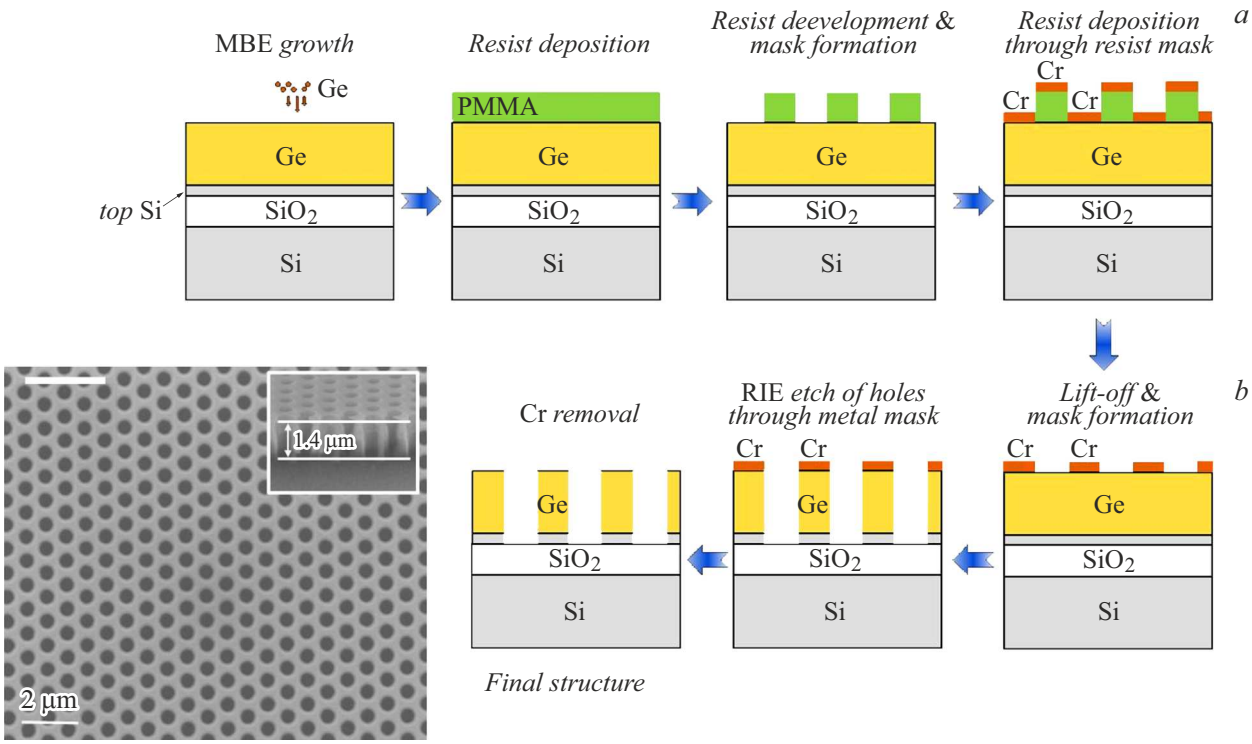

Figure 2. *a* — diagram of the process of forming a structure with PhC. The top layer of Si in SOI substrate with the Si buffer layer, is indicated by a gray rectangle (top Si); *b* — SEM image of one of the fabricated PhC using a metal mask (top view). The insert shows a side view of the chip of one of the PhC, made to determine the total depth of the etched holes.

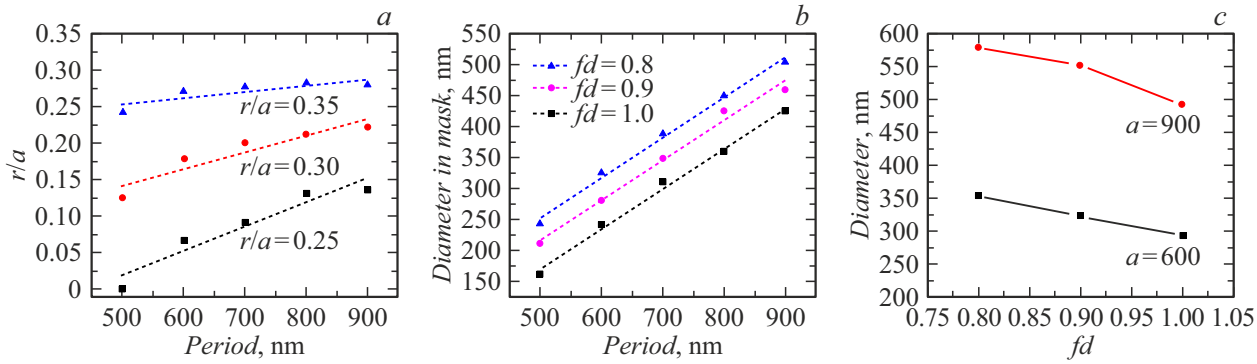

Figure 3. *a* — dependences of the hole diameters obtained in the metal mask (recalculated into ratios r/a) on the PhC period for three values r/a nominally set in the template, which are indicated next to the respective dependencies. Dependences were obtained for the dose correction factor $fd = 0.8$; *b* — dependences of the hole diameters obtained in the metal mask on the PhC period with variation of the dose correction factor fd. The values of fd are listed next to respective dependencies; *c* — dependence of the diameter of the PhC holes in the etched Ge/SOI structure depends on the coefficient fd for two periods, the values of which are indicated next to the respective dependencies. The values are obtained for $r/a = 0.35$ in the template.

fd to 0.7 leads to an insufficient patterning dose for the complete development of the resist.

Fig. 3, *c* shows the dependences of the diameter of PhC holes in Ge/SOI structure after plasma-enhanced chemical etching as a function of the coefficient fd for two periods ($a = 600$ and 900 nm), which demonstrate the possibility of changing the parameters of the PhC holes by changing the dose correction factor. The nominal ratio r/a set in the template was 0.35. It can be seen that the actual diameter values turned out to be less than the required values for all fd, but the smallest deviation was obtained with the minimum of the taken coefficient $fd = 0.8$. Therefore, when using a metal mask, it is necessary to take into account the deviation of the actual diameter of the holes in the structure after RIE etching. Thus, both of the above correction methods can be used to obtain holes with specified parameters when forming PhC in the form of etched holes using a metal mask— both the dose correction

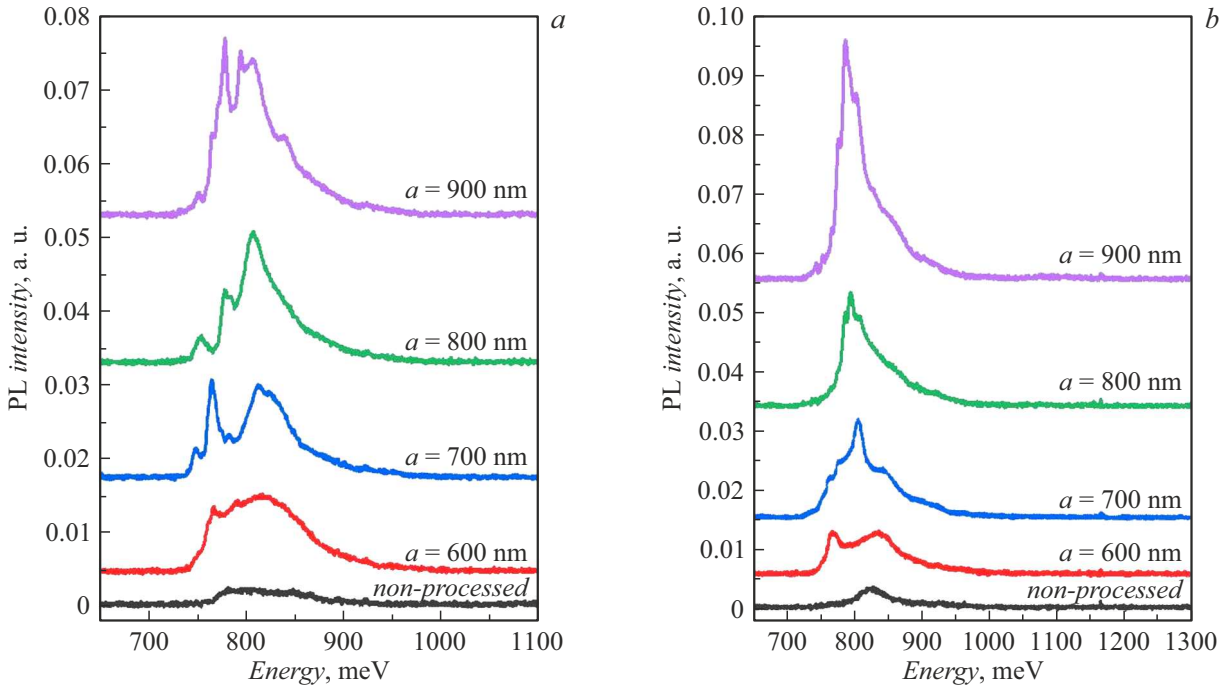

Figure 4. Micro-PL spectra for a set of PhC with different periods indicated next to the respective spectra, and the original region (non-processed) with filling factor values $r/a = 0.29$ (a) and 0.33 (b). All measurements were performed at 300 K.

factor fd and the parameter adjustment in the template for lithography.

As a result, arrays of holes with the required parameters were obtained taking into account the above correction methods which were completely etched through the grown Ge (and Si) layers down to SiO_2 layer, which formed the PhC. As mentioned above, the selectivity of etching the structure with respect to the etching rate of the Cr mask can reach high values due to the low rate of Cr etching in fluorinated plasma [23]. This makes it possible to obtain PhC structures with an etching depth greater than $1\,\mu$m on Ge/SOI. PhC with periods $a = 600-900$ nm and a filling factor $r/a \sim 0.3$ were produced in this study. An example of one of the formed PhC is shown in Fig. 2, *b*. It should be noted that the entire structure is exposed to RIE etching when using a metal mask , except for the PhC area. Therefore, the parameters of the PhC holes can be analyzed using SEM images of the PhC boundary (insert in Fig. 2, *b*). The analysis of SEM images of PhC holes obtained by various methods shows that the verticality of the walls of the holes obtained using a mask made of high contrast resist (Fig. 1, *a*) is better than in the case of usage of a metal mask (Fig. 2, *b*). When using the latter, there is some lateral underetching of the upper part of the Ge layer (i.e., a positive slope of the walls is formed), which may be attributable to the accumulation of charge on the metal surface in the absence of the possibility of its discharge, however, this assumption requires further studies. Another possible reason is the fact that when metal is applied by lift off lithography, almost the entire sample area remains open, while the mask covers only the active area itself (in our case, the PhC area). As a result, the areas around the PhC are etched out during the RIE etching process, which can lead to the appearance of lateral underetching of the edges of the active region.

The photoluminescence spectra of PhC obtained on Ge/SOI structure using a metal mask were studied at room temperature. The results of measurement of the micro-PL spectra at 300 K are shown in Fig. 4 for several PhC with different periods and two values of the filling factor r/a. Also, for comparison, Fig. 4 shows the spectrum from the original Ge/SOI structure without PhC. It can be seen that a significant increase of both the peak and integral intensity of the PL signal from the PhC compared to the initial structure is observed in both cases. The greatest increase of peak intensity is observed with the best spectral correspondence of the PhC mode to the maximum of the PL signal from the initial structure (near 800 meV, which corresponds to the energy of the direct optical transition in Ge). A slight discrepancy is associated with interference effects, since the structures are grown on SOI substrates (see the previous work by the authors of Ref. [38], where a similar effect was observed). The PhC mode structure is more clearly traced for PhC with a smaller r/a, which is expressed in several peaks more clearly discriminated on the PL spectra, however, the presence of several peaks in the spectra is distinguishable in case of large r/a. Quantitative analysis showed that an increase of the peak intensity of PL up to 20 times was observed in the best samples with PhC, and the integral intensity increased up to 17 times compared

with the initial structure without PhC. This fact is associated both with an improvement of the light extraction from the structure due to a violation of the conditions of total internal reflection, and, possibly, with manifestations of the Purcell effect, however, determining the contribution of each of these factors is beyond the scope of this work.

Conclusion

The possibility of using inverse lithography to form a metal mask on samples based on Ge layers grown on SOI substrates was studied in the paper. The technology of forming a metal mask in combination with ICP RIE has been developed, which makes it possible to form deep (more than $1\,\mu$m) holes in Ge/Si material. A comparison of the proposed method with the use of a specialized high contrast electron-beam resist for RIE showed the achievability of comparable etching depths, albeit with a slightly worse wall verticality of the holes. Nevertheless, a potential usage of a metal mask when it is necessary to obtain large etching depths with small pattern elements may be more promising, because a high contrast resist still has limited selectivity, although it exceeds selectivity of standard electron-beam resists. The possibilities of this method were confirmed by forming photonic crystals on Ge/SOI layers and demonstrating an increase of the PL signal from such structures by more than an order of magnitude.

Funding

The work has been performed under state assignment of IPM RAS (FFUF-2024-0019). Part of the work related to electron beam lithography was supported within the framework of the state assignment of the Institute of Physical Problems of SB RAS.

Acknowledgments

The authors would like to thank the Common Use Center „Physics and Technology of Micro- and Nanostructures“ of Institute for Physics of Microstructures, Russian Academy of Sciences), Common Use Center „Nanostructures“ of Institute of Physical Problems of SB RAS and Common Use Center of VTAN NSU for providing opportunities to use technological equipment.

Conflict of interest

The authors declare that they have no conflict of interest.

References

[1] A.I. Kuznetsov, A.E. Miroshnichenko, M.L. Brongersma, Y.S. Kivshar, B. Lukyanchuk. Science, 354, aag2472 (2016). DOI: 10.1126/science.aag2472

[2] K. Koshelev, Y. Kivshar. ACS Photon, **8**, 102 (2021). DOI: 10.1021/acsphotonics.0c01315

[3] O.A.M. Abdelraouf, Z. Wang, H. Liu, Z. Dong, Q. Wang, M. Ye, X.R. Wang, Q.J. Wang, H. Liu. ACS Nano, **16**, 13339 (2022). DOI: 10.1021/acsnano.2c04628

[4] A.I. Kuznetsov, M.L. Brongersma, J. Yao, M.K. Chen, U. Levy, D.P. Tsai, N.I. Zheludev, A. Faraon, A. Arbabi, N. Yu, D. Chanda, K.B. Crozier, A.V. Kildishev, H. Wang, J.K.W. Yang, J.G. Valentine, P. Genevet, J.A. Fan, O.D. Miller, A. Majumdar, J.E. Fröch, D. Brady, F. Heide, A. Veeraraghavan, N. Engheta, A. Alù, A. Polman, H.A. Atwater, P. Thureja, R. Paniagua-Domínguez, S.T. Ha, A.I. Barreda, J.A. Schuller, I. Staude, G. Grinblat, Yu. Kivshar, S. Peana, S.F. Yelin, A. Senichev, V.M. Shalaev, S. Saha, A. Boltasseva, Ju. Rho, D.K. Oh, J. Kim, J. Park, R. Devlin, R.A. Pala. Roadmap for Optical Metasurfaces, ACS Photonics, **11**, 816 (2024). DOI: 10.1021/acsphotonics.3c00457

[5] P. Moitra, X. Xu, R. Maruthiyodan Veetil, X. Liang, T.W.W. Mass, A.I. Kuznetsov, R. Paniagua-Domínguez. ACS Nano, **17**, 16952 (2023). DOI: 10.1021/acsnano.3c04071

[6] M. Yoshida, S. Katsuno, T. Inoue, J. Gelleta, K. Izumi, M. De Zoysa, K. Ishizaki, S. Noda. Nature, **618**, 727 (2023). DOI: 10.1038/s41586-023-06059-8

[7] V. Mylnikov, S.T. Ha, Zh. Pan, V. Valuckas, R. Paniagua-Domínguez, H.V. Demir, A.I. Kuznetsov. ACS Nano, **14**, 7338 (2020). DOI: 10.1021/acsnano.0c02730

[8] W. Song, X. Liang, Sh. Li, D. Li, R. Paniagua-Domínguez, K.H. Lai, Q. Lin, Y. Zheng, A.I. Kuznetsov. Laser Photonics Rev., **15**, 2000538 (2021). DOI: 10.1002/lpor.202000538

[9] K. Takeda, T. Tsurugaya, T. Fujii, A. Shinya, Y. Maeda, T. Tsuchizawa, H. Nishi, M. Notomi, T. Kakitsuka, S.H. Matsuo. Opt. Expr., **29**, 26082 (2021). DOI: 10.1364/OE.427843

[10] E. Dimopoulos, A. Sakanas, A. Marchevsky, M. Xiong, Y. Yu, E. Semenova, J. Mørk, K. Yvind. Laser Photonics Rev., **16**, 2200109 (2022). DOI: 10.1002/lpor.202200109

[11] A. Shakoor, R.L. Savio, P. Cardile, S.L. Portalupi, D. Gerace, K. Welna, S. Boninelli, G. Franzò, F. Priolo, Th.F. Krauss, M. Galli, L. O'Faolain. Laser Photonics Rev., **7**, 114 (2013). DOI: 10.1002/lpor.201200043

[12] A. Mahdavi, G. Sarau, J. Xavier, T.K. Paraïso, S. Christiansen, F. Vollmer. Sci. Rep., **6**, 25135 (2016). DOI: 10.1038/srep25135

[13] J.S. Xia, Y. Ikegami, Y. Shiraki, N. Usami, Y. Nakata. Appl. Phys. Lett., **89**, 201102 (2006). DOI: 10.1063/1.2386915

[14] P. Boucaud, M. El Kurdi, S. David, X. Checoury, X. Li, T.-P. Ngo, S. Sauvage, D. Bouchier, G. Fishman, O. Kermarrec, Y. Campidelli, D. Bensahel, T. Akatsu, C. Richtarch, B. Ghyselen. Thin Solid Films, **517**, 121 (2008). DOI: 10.1016/j.tsf.2008.08.146

[15] R. Jannesari, M. Schatzl, F. Hackl, M. Glaser, K. Hingerl, T. Fromherz, F. Schäffler. Opt. Expr., **22** (21), 25426 (2014). DOI: 10.1364/OE.22.025426

[16] V. Rutckaia, F. Heyroth, A. Novikov, M. Shaleev, M.I. Petrov, J. Schilling. Nano Lett., **17** (11), 6886 (2017). DOI: 10.1021/acs.nanolett.7b03248

[17] S.A. Dyakov, M.V. Stepikhova, A.A. Bogdanov, A.V. Novikov, D.V. Yurasov, M.V. Shaleev, Z.F. Krasilnik, S.G. Tikhodeev, N.A. Gippius. Laser Photonics Rev., **15** (7), 2000242 (2021). DOI: 10.1002/lpor.202000242

[18] R.W. Millar, K. Gallacher, J. Frigerio, A. Ballabio, A. Bashir, I. MacLaren, G. Isella, D.J. Paul. Opt. Expr., **24** (5), 4366 (2016). DOI: 10.1364/OE.24.004365

[19] V. Rutckaia, F. Heyroth, G. Schmidt, A. Novikov, M. Shaleev, R. Savelev, J. Schilling, M. Petrov. ACS Photon., **8**, 209 (2021). DOI: 10.1021/acsphotonics.0c01319
[20] A.V. Miakonkikh, A.V. Shishlyannikov, A.A. Tatarintsev, V.O. Kuzmenko, K.V. Rudenko, E.S. Gornev. Russ. Microelectron., **50**, 297 (2021). DOI: 10.1134/S1063739721050048
[21] Electronic media. Available at: https://www.aqmaterials.com/aqm-silsesquioxane-polymers
[22] V.A. Volodin, V.A. Zinovyev, Zh.V. Smagina, A.F. Zinovieva, E.E. Rodyakina, A.V. Kacyuba, K.N. Astankova, K.V. Baryshnikova, M. Petrov, M.S. Mikhailovskii, M.V. Stepikhova, V.A. Verbus, A.V. Novikov. Photonics, **10**, 1248 (2023). DOI: 10.3390/photonics10111248
[23] V.M. Donnelly, A. Kornblit. J. Vac. Sci. Technol., **A31**, 050825 (2013). DOI: 10.1116/1.4819316
[24] S. Wu, H. Xia, J. Xu, X. Sun, X. Liu. Adv. Mater., **47**, 1803362 (2018). DOI: 10.1002/adma.201803362
[25] A. Goodyear, M. Boettcher, I. Stolberg, M. Cooke. Proc. SPIE 9428, 94280V-1 (2015). DOI: 10.1117/12.2085469
[26] A.V. Peretokin, D.V. Yurasov, M.V. Stepikhova, M.V. Shaleev, A.N. Yablonskiy, D.V. Shengurov, S.A. Dyakov, E.E. Rodyakina, Zh.V. Smagina, A.V. Novikov. Nanomaterials, **13**, 1678 (2023). DOI: 10.3390/nano13101678
[27] R. Geiger, T. Zabel, H. Sigg. Front. Mater., **2**, 52 (2015). DOI: 10.3389/fmats.2015.00052
[28] J. Liu, X. Sun, R. Camacho-Aguilera, L.C. Kimerling, J. Michel. Opt. Lett., **35** (5), 679 (2010). DOI: 10.1364/ol.35.000679
[29] J. Liu, X. Sun, D. Pan, X. Wang, L.C. Kimerling, Th.L. Koch, J. Michel. Opt. Exp., **15**, 11272 (2007). DOI: 10.1364/oe.15.011272
[30] S. Wirths, R. Geiger, N. von den Driesch, G. Mussler, T. Stoica, S. Mantl, Z. Ikonic, M. Luysberg, S. Chiussi, J.M. Hartmann, H. Sigg, J. Faist, D. Buca, D. Grützmacher. Nat. Photon., **9**, 88 (2015). DOI: 10.1038/nphoton.2014.321
[31] A. Elbaz, D. Buca, N. von den Driesch, K. Pantzas, G. Patriarche, N. Zerounian, E. Herth, X. Checoury, S. Sauvage, I. Sagnes, A. Foti, R. Ossikovski, J.-M. Hartmann, F. Boeuf, Z. Ikonic, P. Boucaud, D. Grutzmacher, M. El Kurdi. Nat. Photon., **14**, 375 (2020). DOI: 10.1038/s41566-020-0601-5
[32] D. Buca, A. Bjelajac, D. Spirito, O. Concepciyn, M. Gromovyi, E. Sakat, X. Lafosse, L. Ferlazzo, N. von den Driesch, Z. Ikonic, D. Grutzmacher, G. Capellini, M. El Kurdi. Adv. Opt. Mater, **10** (22), 2201024 (2022). DOI: 10.1002/adom.202201024
[33] F.T. Armand Pilon, A. Lyasota, Y.-M. Niquet, V. Reboud, V. Calvo, N. Pauc, J. Widiez, C. Bonzon, J.-M. Hartmann, A. Chelnokov, J. Faist, H. Sigg. Nature Commun., **10**, 2724 (2019). DOI: 10.1038/s41467-019-10655-6
[34] J.M. Hartmann, A. Abbadie, J.P. Barnes, J.M. Fedeli, T. Billon, L. Vivien. J. Cryst. Growth, **312**, 532 (2010). DOI: 10.1016/j.jcrysgro.2009.11.056
[35] V.A. Shah, A. Dobbie, M. Myronov, D.R. Leadley. Thin Solid Films, **519**, 7911 (2011). DOI: 10.1016/j.tsf.2011.06.022
[36] O. Skibitzki, M.H. Zoellner, F. Rovaris, M.A. Schubert, Y. Yamamoto, L. Persichetti, L. Di Gaspare, M. De Seta, R. Gatti, F. Montalenti, G. Capellini. Phys. Rev. Mater., **4**, 103403 (2020). DOI: 10.1103/PhysRevMaterials.4.103403
[37] Yu.B. Bolkhovityanov, L.V. Sokolov. Semicond. Sci. Technol., **27**, 043001 (2012). DOI: 10.1088/0268-1242/27/4/043001
[38] D.V. Yurasov, A.N. Yablonskiy, N.A. Baidakova, M.V. Shaleev, E.E. Rodyakina, S.A. Dyakov, A.V. Novikov. J. Phys. D: Appl. Phys., **55**, 075107 (2022). DOI: 10.1088/1361-6463/ac32fe
[39] H.-C. Luan, D.R. Lim, K.K. Lee, K.M. Chen, J.G. Sandland, K. Wada, L.C. Kimerling. Appl. Phys. Lett., **75**, 2909 (1999). DOI: 10.1063/1.125187
[40] D.V. Yurasov, A.I. Bobrov, V.M. Daniltsev, A.V. Novikov, D.A. Pavlov, E.V. Skorokhodov, M.V. Shaleev, P.A. Yunin. Semiconductors, **49** (11), 1415 (2015). DOI: 10.1134/S1063782615110263
[41] Electronic media. Available at: https://www.allresist.com/portfolio-item/e-beam-resist-ar-p-6200-series-csar-62/

Translated by A.Akhtayamov